Journal of the European Ceramic Society 16 (1996) 483–491

0955-2219(95)00160-3
0955-2219/96/$15.00

Wet Erosive Wear Behaviour of Fine-grain Zircon Ceramic

A. Wootton, M. Miranda-Martinez,* R. W. Davidge & F. L. Riley†

School of Materials, University of Leeds, Leeds LS2 9JT, UK

(Received 27 January 1995; revised version received 4 August 1995; accepted 27 August 1995)

Abstract

The wet erosive wear rates of a set of hot-pressed, dense, fine-grained zircon materials of grain size in the range 2 to 6 μm have been measured. There is no correlation between wear rate and hardness or fracture toughness: wear rate instead appears to be strongly linked to grain size and pore fraction. The wear rate–grain size relationship is explicable in terms of a model based on grain-boundary microfracture and crack linking, which allow grain detachment to occur. Wear rates for this set of zircon materials are slightly lower than those measured for a set of pure polycrystalline aluminas with a similar grain size range.

1 Introduction

Zircon (zirconium silicate, $ZrSiO_4$) is widely used as the constituent of many traditional ceramic materials, refractories and glazes,[1–6] and there is interest in its use as a basis for milling media because of its hardness and low cost. At high temperature (~1675°C) zircon dissociates into zirconium dioxide and silicon dioxide,[7,8] but by the use of liquid forming sintering additives it is possible to densify zircon powder at relatively low temperatures with retention of the zircon phase.[9–11]

Zircon has a hardness of ~7·5 on the Mohs scale,[6] and although this is significantly less than that of alumina [~9, corresponding to a Vickers indentation hardness of ~25 GPa (Ref. 12)] zircon-based materials might be expected to be reasonably wear resistant. For the milling application considered wet erosion resistance is of primary importance, and this wear mode was assessed during the preliminary investigation reported here. Wear testing was carried out using laboratory equipment, with a set of dense zircon discs of tailored grain size and controlled porosities, obtained by hot-pressing zircon powder in the presence of a siliceous liquid phase. The $CaO–MgO–SiO_2$ system was used as densification aid, because it provides a suitable liquid at < 1300°C.[8]

Many attempts have been made to model the wear behaviour of brittle ceramics in terms of the parameters which intuitively seem likely to control wear, and which can be justified on the basis of a fracture mechanics approach. Several of these have led (see, for example, ref. 13) to the development of equations of the general form:

$$V \propto P^a H^{-b} K^{-c} \quad (1)$$

in which the volume of material removed (V) is related to the applied load (P), hardness (H) and fracture toughness (K), for which in this particular instance the exponents are given by $a = 5/4$, $b = 1/2$ and $c = 3/4$. It would be expected, and is indeed found, that in general good wear resistance is obtained in materials which have high hardness and fracture toughness, and over a broad range of materials types convincing correlations are found.

However, this type of expression has its limitations in that it takes into account only three possible wear controlling parameters, and other possibilities, such as the electrical effects noted in insulating materials during dry sliding,[14] are disregarded. These limitations become particularly apparent when comparing the members of a specific class of material (such as the aluminas, and the zircons examined here) for which differences in hardness are small, and the effects of microstructure on toughness not clear. A number of arguments can be advanced to show that such a simple type of relationship is not appropriate for accounting for the differences in wear rates observed in these cases. For example, correlations between wear resistance and toughness for pure and liquid-phase sintered aluminas are poor, and variations of crack propagation resistance with crack length (R-curve behaviour) might be expected to influence wear behaviour.[15] However, although coarse-grained alumina shows marked R-curve behaviour this is

* Now at ISQ, Lisbon, Portugal.
† To whom correspondence should be addressed.

not necessarily an advantage when the critical wear events occur over dimensions of a single grain. A similar problem exists with the application of hardness data obtained from the use of an indenter giving penetration over many grain dimensions, and doubts have been expressed about the appropriateness of such data. Within a specific class of material other factors must operate to provide differences in wear rate, and microstructure very clearly is an important one. For materials of normal grain size a strong influence of grain size has been found in a wide range of wear modes, with low rates associated with fine grain size. For many wear modes, ranging from sliding to grinding and cutting, wear rate is observed to vary as a function of (grain size)$^{-n}$, where n commonly approximates to 1/2.[16–23] These relationships have in general been attributed either to residual grain boundary stress (native to anisotropic materials such as alumina), or to the presence of defects, the size of which scales with the grain size. It seems clear, however, that the basis for the wear process must reside at the sub-grain level, even though the observed material loss process commonly consists of the detachment of whole grains. For very fine grained materials (< 1 μm) polishing seems to be the preferred wear mechanism, and it is likely that in these cases an underlying tribochemical wear mechanism becomes the dominant process, albeit at a very slow overall rate.

Recently, a tentative model has been presented for the wear of polycrystalline materials of grain sizes in the range 1 to 12 μm,[24] which makes the assumption that in the mechanical component of the wear process fracture occurs predominantly along two-grain boundaries (that is, the grain faces), with cracks progressing along individual grain faces at a mean rate characteristic of the material. There is then a delay in crack propagation, for readjustment of the direction of propagation, at each three-grain junction.

The time (t) for the crack to progress a specified distance (d) is given by:

$$t = 2\,(t_f + t_j).d/G \tag{2}$$

where t_f is the time (proportional to the mean grain dimension, G) to traverse a two-grain boundary face of dimension ~G/2, and t_j is the time (a constant) taken to realign at a three-grain junction. The experimentally observed wear rate (W) is thus:

$$W = Ad/t \tag{3}$$

or

$$W = AG/2\,(t_f + t_j) \tag{4}$$

where A is a constant related to the microstructural crack linking process and the experimental conditions of the test. t_f can be eliminated by defining a characteristic grain size (G_o) for which $t_f = t_j$. Thus:

$$t_f = (G/G_o)\,t_j \tag{5}$$

and substitution into (4) gives

$$W = A\,G\,G_o/[2t_j(G + G_o)] \tag{6}$$

A proportionality between W and $G/(G + G_o)$ is thus predicted, with the plot passing through the origin. This prediction has been shown to be supported by a wide range of wear data for which the value of G_o ranges from 1 to 100 μm, depending on the nature of the wear process. G_o is expected to vary with the nature of the wear process and conditions, which affect in particular the scale of the damage and the way that individual cracks link to form a chip. This wear model specifically focuses on grain size effects and ignores possible contributions from other material removal processes not likely to be grain size dependent, such as tribochemical wear. It is therefore considered to be applicable to materials with grain size above a lower limit of ~1 μm. An upper limit cannot at present be identified, though the wear rates of a material of infinite grain size (single crystal sapphire) are generally much slower than the simple extrapolation of the essentially polycrystalline model would predict. The precise details of the mechanisms of the grain-boundary crack nucleation and propagation processes are of necessity at this stage undefined.

2 Experimental

Dense zircon materials were prepared from a premium grade Australian zircon sand (R.Z.M. Premium B). This was ball milled in water using alumina media to give a set of four powders with mean particle sizes in the range 1·7 to 8·7 μm. Particle size determinations were carried out on aqueous suspensions using a Coulter LS130 Laser Diffraction Particle Size Analyzer, with 0·2% Dispex N40 (Allied Colloids, Bradford) dispersant. Chemical analysis of the milled powders obtained by X-ray fluorescence (Philips model 1606) on fused borate glass discs showed that appreciable levels of alumina were introduced during the milling, with the maximum quantity in the longest milled, and finest, zircon powder (Z1). In order to obtain the same overall composition for each of the four powders, varying amounts of alumina were added to powders Z2, Z3 and Z4, as the equivalent amounts of the isopropanol soluble aluminium nitrate (Aldrich Chemical Co. Ltd), to bring the total up to that of powder Z1 (4·24%).

A liquid-forming densification aid corresponding to the composition $CaO–MgO–2SiO_2$, at the level of 8% by weight, was blended by wet mixing into each powder using appropriate quantities of calcium and magnesium nitrates (Aldrich Chemical Co. Ltd, or BDH Chemicals, Poole) and ultra-fine silicon dioxide powder (Aerosil 380, Degussa AG, Frankfurt). Thermogravimetric analysis established the dry oxide equivalent for each additive. Each powder blend was mixed in isopropanol for 2 h using zirconia media, and then dried at 30°C under low pressure in a rotary evaporator to avoid melting the nitrates. Dried powders were lightly crushed, sieved through a 100 μm aperture nylon sieve, calcined in alumina crucibles at 700°C for 1 h, and then crushed and re-sieved.

Powders were hot-pressed to high density in a 25 mm bore graphite die, with powder sufficient to give a final disc thickness of 5 mm. Temperature, pressure and die punch movement were continuously monitored and data processed by computer to provide a measure of extent of densification as a function of time. Trial hot-pressings on the three finer powders (Z1, Z2, and Z3) established their optimum conditions of 1375°C and 20 MPa, and times between 0·5 and 2 h. Onset of liquid formation (and of rapid densification) occurred at ~1300°C. The coarsest powder (Z4) was hot-pressed under varying conditions, to give a second set of materials of mean grain size 6·2 μm, with a range of densities and thus residual porosities.

Discs of hot-pressed materials were cleaned with SiC powder, sectioned, and polished to 1 μm diamond for examination by X-ray diffraction (XRD), and by scanning electron microscopy (SEM) (Cambridge Instruments Camscan models 3 and 4) with a Link X-ray microanalysis system attachment. Mean zircon grain sizes were measured from photographs of polished and thermally etched materials, using the standard line intercept technique, and counting a minimum of 600 grains. The composition of the material was estimated by analyses of areas using point counting and line intercept measurements and the multiplication factor 1·56.[25]

Disc densities were measured by the standard water immersion technique (BS 7134 Section 1.2). Theoretical (true solid) density values (ρ) for the dense materials were obtained using powder crushed to pass through a 100 μm sieve and immersed in deionized water, on the basis of BS 7134. Microindentation hardness (H) and fracture toughness (K_{1c}) were measured on polished faces, by Vickers indentation with a load of 29 N, and the equation of Anstis *et al.*[26]

Wet erosion was carried out in a modified high torque attritor mill using 0·5 to 1 mm dimension crushed fused alumina aggregate in water. A detailed description of the wear test has been given.[23,27] Zircon discs 25 mm diameter and ~5 mm thick were clamped between shaped discs of hard polyurethane attached to the shaft of the mill, with ~50% of the zircon disc exposed. The sample holder was immersed in a slurry consisting of 700 g of alumina grit (of stated purity 92·2% Al_2O_3, with SiO_2 and TiO_2 as the major impurities) in 250 cm^3 of deionised water, and rotated at a speed of 8 Hz with a disc track radius of 36 mm (giving a disc perimeter linear velocity of ~1·9 m s^{-1}). Disc weights to ± 0·1 mg were measured after 2 h (t_1) and 6 h (t_2) testing (w_1 and w_2), using the standardized procedure. A wear rate (R) measured in m s^{-1} was calculated on the basis of the expression:

$$R = [(w_1–w_2) / (t_2–t_1)]/(A\rho)$$

where A is the area of the exposed leading quadrant of the disc (approximately 1/4 of the disc surface area). This time period was chosen in order to minimize any effects of the disc's initial surface finish, and the significant smoothing of the grit particles at longer times. Worn surfaces were examined by SEM. Each disc generally provided two wear values, and these were averaged.

3 Results

Table 1 shows the chemical compositions of the four zircon powders after milling; a 'balanced' composition Z1 was used as the basis for the zircon materials used. Analysis also showed the presence in the powders of small amounts of CaO (0·12%) and MgO (0·08%), possibly, introduced by the milling media, and these amounts were taken into account in the calculation of the weights of liquid-forming sintering additives used. Figures 1(a) to (d) show the frequency distribution curves for the four zircon starting powders. Figure 2 shows a typical scanning electron micrograph of the Z2 powder of mean size 2.7 μm. The hot-pressing conditions chosen initially (1375°C and 20 MPa) and found to be satisfactory for the three finest powders, are shown in Table 2, together with the resulting mean grain sizes and densities. The hot-pressing densification conditions for powder

Table 1. Chemical composition (weight%) of milled zircon powders: compositions used for hot-pressing were adjusted to give that of composition Z1

Powder	*Median dimension (μm)*	*ZrO_2*	*HfO_2*	*SiO_2*	*Al_2O_3*
Z1	1·4	62·1	1·3	32·4	4·3
Z2	2·0	63·8	1·3	32·5	2·4
Z3	3·8	63·7	1·3	32·3	2·7
Z4	7·3	63·4	1·3	33·3	2·0

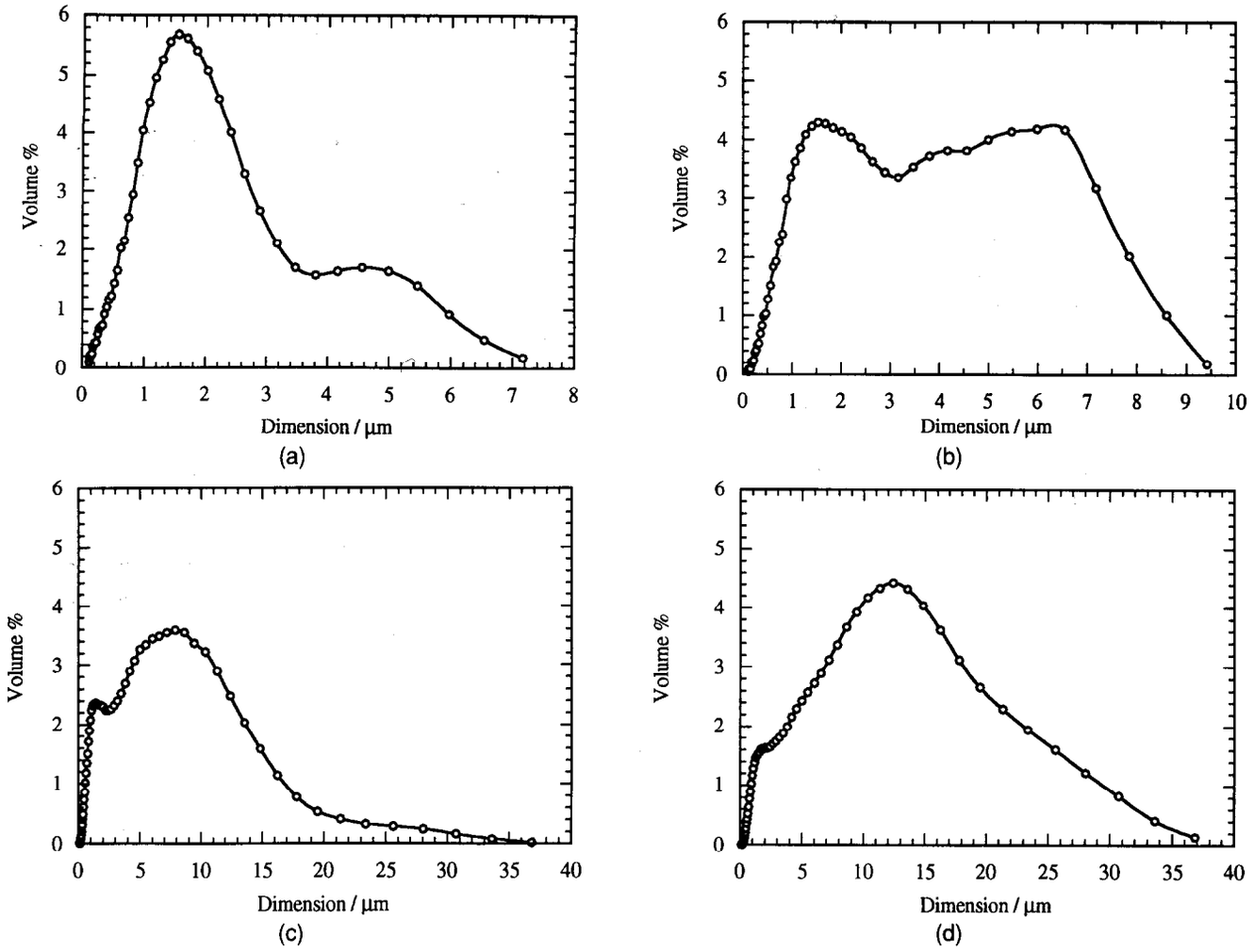

Fig. 1. Frequency distribution curves for the four milled zircon powders, of the computed median dimensions: (a) Z1, 1·4 μm; (b) Z2, 2·0 μm; (c) Z3, 3·8 μm; (d) Z4, 7·3 μm.

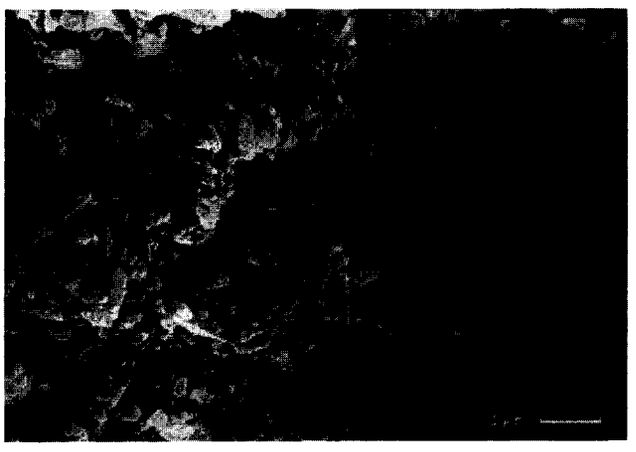

Fig. 2. A scanning electron micrograph of the 2·7 μm zircon powder.

Table 2. Hot-pressing conditions and material densities (temperature 1375°C; pressure 20 MPa)

Material	*Time (h)*	*Mean grain size (μm)*	*Bulk density (Mg m^{-3})*	*%Theoretical*
Z1	0·5	2·8 ± 0·2	4·35 ± 0·01	98·9
Z2	0·5	4·2 ± 0·3	4·32 ± 0·01	98·2
Z3	1·0	5·2 ± 0·3	4·40 ± 0·01	100·0
Z4.2	1·0	6·2 ± 0·3	4·24 ± 0·01	96·4

Z4, and material densities and grain sizes, are given in Tables 3(a) and 3(b) respectively. Table 4 shows hardness and fracture toughness data for the four most dense materials.

It was clear from the micrographs, and the relationship between initial powder mean particle size and the corresponding mean grain size of the derived materials (Fig. 3), that the hot-pressing

Table 3(a). Hot-pressing conditions for the set of 8·7 μm based zircon powder materials

Material	*Pressure (MPa)*	*Temperature (°C)*	*Time (h)*
Z4.1	10	1350	0·8
Z4.2	20	1375	1·0
Z4.3	10	1450	1·1

Table 3(b). Z4 densities and porosities

Material	*Grain size (μm)*	*Bulk density (Mg m^{-3})*	*Pore fraction*
Z4.1	6·2 ± 0·3	4·03 ± 0·01	0·084
Z4.2	6·2 ± 0·3	4·24 ± 0·01	0·036
Z4.3	6·2 ± 0·3	4·34 ± 0·01	0·014

Table 4. Property data for dense zircon materials

Material	*Grain size (μm)*		*Hardness (GPa)*	K_{Ic} *(MPa m$^{1/2}$)*
Z1	2·8 ± 0·5		10·6 ± 1·0	2·9 ± 0·3
Z2	4·2 ± 0·5		10·2 ± 1·0	2·3 ± 0·3
Z3	5·2 ± 0·5		10·9 ± 1·0	2·1 ± 0·3
Z4.3	6·2 ± 0·5		10·3 ± 1·0	2·6 ± 0·3
		mean	10·5 ± 1·0	2·5 ± 0·3

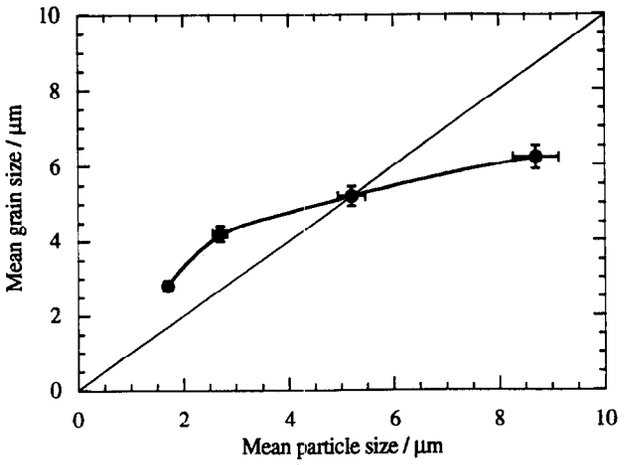

Fig. 3. Mean grain size of dense materials as a function of mean zircon partlcle size.

technique had been successful in giving high densities with no significant grain growth. Figure 4 shows a typical back-scattered electron micrograph of dense material Z1 obtained by hot-pressing at 1375°C for 0·5 h. Figure 5 shows fully dense Z4.3 (6·2 μm grain size), after hot-pressing at 1450°C for 1·1 h. The grey areas were shown by EDS analysis to be zircon; the white regions of dimension 0·5–1 μm for Z1 and 1–3 μm for Z4·3 (determined by the line intercept method) contained predominantly Zr with small amounts of Ca, indicating that they were zirconia with solid-solution calcium oxide. Analyses of the phase areas in all dense materials by point counting and line

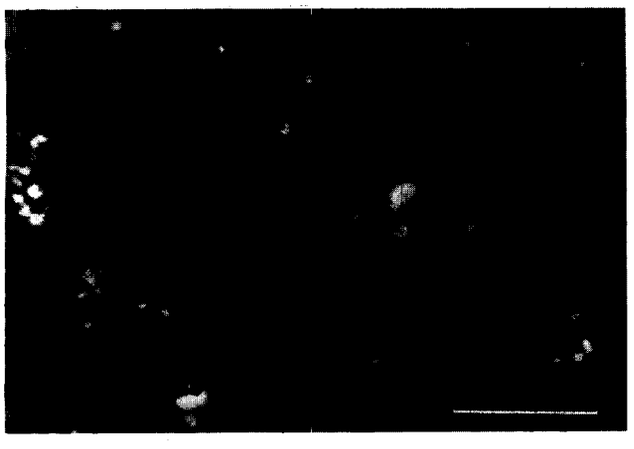

Fig. 4. A back-scattered electron micrograph of material of Z1 (mean grain size 2·8 μm); white regions zirconia, grey regions zircon.

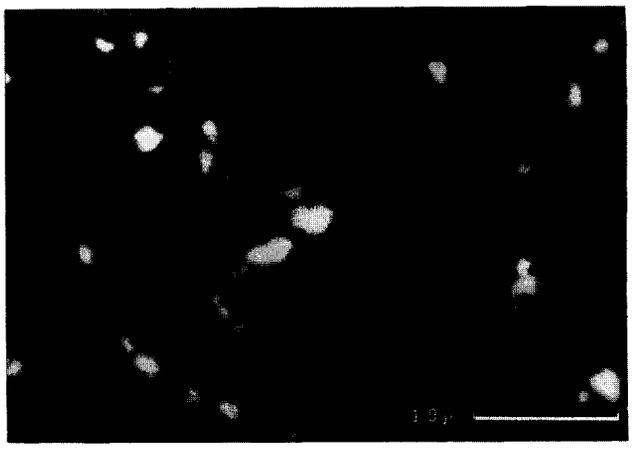

Fig. 5. A back-scattered electron micrograph of material Z4.2 (mean grain size 6·2 μm); white regions zirconia, grey regions zircon.

Table 5. Wear rate data for all zircon materials

Material	*Grain size (μm)*	*Pore fraction*	*Wear rate (nm s^{-1})*
Z1	2·8	<0·02	26
Z2	4·2	<0·02	31
Z3	5·2	<0·02	36
Z4.1	6·2	0·082	58
Z4.2	6·2	0·036	53
Z4.3	6·2	0·014	35

intercept measurements showed that the mean zirconia content was ~2·5% and the mean glass content ~21%; there was no obvious trend with powder particle size or hot-pressing conditions.

Wear tests were carried out on 25 mm discs of all materials using the standard conditions. Mean wear rate data derived from the weight losses between 2 and 6 h of wearing are given in Table 5. Repeated measurements of wear rates for the same disc using different disc quadrants showed that the R values were constant within ±3%.

Wear rates as a function of mean grain size are shown in Fig. 6, and wear rate as function of

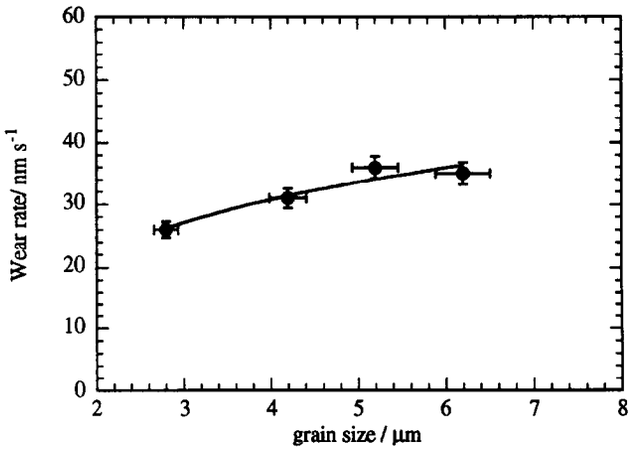

Fig. 6. Wear rate as a function of mean grain size.

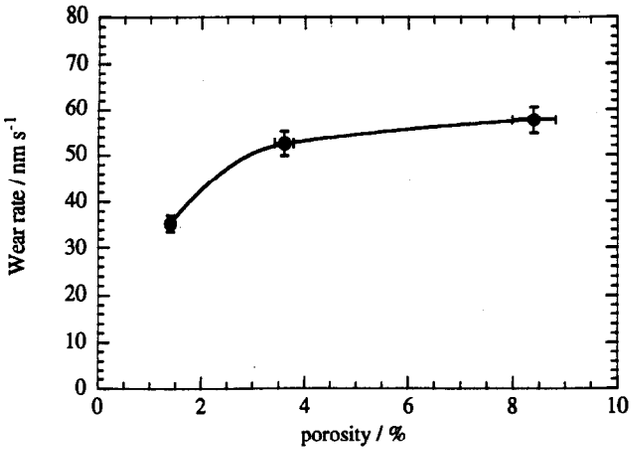

Fig. 7. Wear rate as function of porosity.

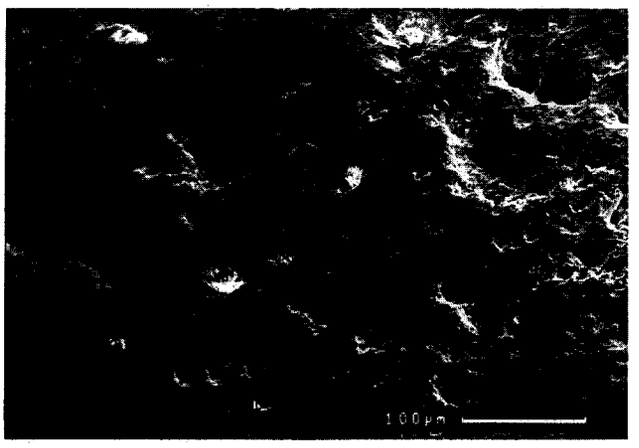

Fig. 8. A scanning electron micrograph of a disc of porous Z4.1 material after 6 h wear.

Fig. 9. A scanning electron micrograph of the edge of a disc of Z4.1 material after 6 h wear.

porosity is shown in Fig. 7. Figures 8, 9 and 10 show typical views of the surface structures of worn discs. Fig. 8, at lower magnification, shows the extensive wear taking place in the vicinity of porosity after 6 h wear. Figure 9, of the dense material, provides strong evidence for grain detachment. Figure 10, at higher magnification, shows for a smoother section of the surface the relief polishing effects, with the loss of some grains by detachment.

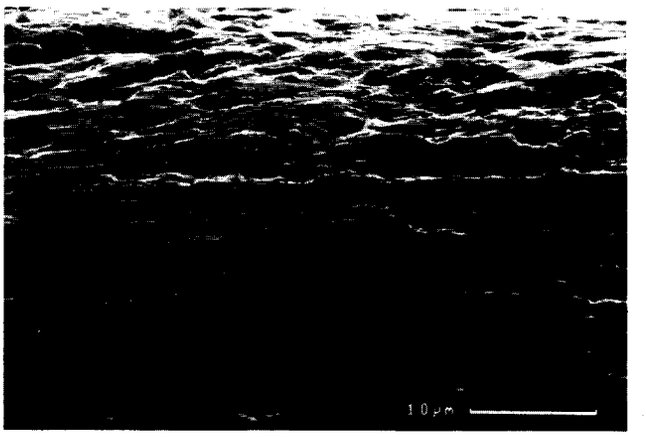

Fig. 10. A scanning electron micrograph of a disc of Z4.2 material after 6 h wear.

4 Discussion

The zircon powders had a trend towards bimodal size distribution, which was most marked for the two intermediate size powders Z2 and Z3. This results in the tendency, shown clearly in the SEM micrographs of Z2 powder in Fig. 2, for very small (~1 μm) fragments to split off from large (~10 μm) particles during milling. Nonetheless, the spread of the four median sizes was sufficiently wide that the powders could be regarded as having an identifiable mean dimension. Coefficients of variation, defined as standard deviation/mean particle dimension, were in the range 0·72 to 0·93.

During hot-pressing an appreciable proportion of the zircon powder (likely to be mainly the finer particle size fraction) dissolves in the aluminosilicate liquid to yield the large (~21 %) volume of siliceous liquid, seen as a glass phase in the dense material. EDS analysis showed this glass to contain relatively small amounts of Ca and Al, and a very much larger proportion of Si and Zr, confirming the dissolution of a significant amount of zircon into the liquid. The overall system is very complex, but viewed at the simplest level the incorporation of the 'impurity' Al_2O_3 into the silicate system will generate liquids of lower forming temperature than those in the simple CaO–MgO–$2SiO_2$ system; certainly at temperatures well below the melting point of diopside ($CaO.MgO{\cdot}2Al_2O_3$) of 1392°C and probably lower than that of the 1170°C eutectic in the Al_2O_3–CaO–SiO_2 system. During densification very little direct fusion by sintering of the zircon grains occurs, and even after 1 h at 1450°C there is no significant grain growth; the correlation between starting zircon median particle size and measured mean grain size in the dense materials is close (Fig. 3). Some shift of median particle size occurs because a greater proportion of fines is likely to be lost by dissolution; in addition,

the fundamentally different techniques used in the estimations of the two dimensions have to be taken into account. Figures 4 and 5 show that there is only a small amount of direct bridging of the zircon grains at the original particle contact points; the glass is therefore generally the continuous phase. An estimated 2·5% by volume of very fine (<~1 μm) zirconia particles develops. These zirconia particles are well distributed in the material, in a pattern which is independent of zircon particle size. It appears that they nucleate and develop at zircon surfaces during the release of an equivalent proportion of silica into the liquid phase. Some apparent bridging of zircon particles by zirconia particles can also be seen. The zirconia particles were assumed to be the cubic, fully stabilized ZrO_2 phase, but this was not firmly established.

The microindentation hardness (mean 10·5 ± 1·0 GPa) and fracture toughness (mean 2·5 ± 0·3 MPa $m^{1/2}$) values are independent of zircon grain size. The relatively low hardness values are assumed to be the consequence of the large volume of glass present in these materials.

There is clearly no relationship between wear rate and hardness or fracture toughness within this set of materials. The wear surfaces were in general fairly smooth, with some local roughening delineated by the zircon grain edges. There was very severe, localized pitting in coarser grain size materials, and particularly in those containing higher levels of porosity. In the smooth surface regions grain outlines are just visible, and differences in wear rate between the zircon grains and intergranular glass were not marked. This general impression of a polishing effect suggests that another, quite different, process such as the tribochemical loss of material is contributing to wear, by superposition on an underlying mechanical wear process involving grain fracture. Grain facetting seen on the flatter surfaces, and the large extents of wear at pore shoulders, indicate that whole grain detachment is also occurring.

The overall wear rate is clearly related to grain size (Fig. 6) and, at this stage of the investigation of the erosive wear of polycrystalline materials of this type, emphasis has been placed on developing an understanding of the relationship between grain size and the probability of grain detachment, in the context of a wear process largely initiated by the point impact of a grit particle on a surface. For polycrystalline alumina materials with mean grain size less than ~2 μm, tribochemical polishing appeared to be the major wear mechanism.[23] In the case of the polycrystalline zircon materials examined here, because the finest grain size was of the order of 3 μm, it would be expected that tribochemical wear might not be an important component of the erosive wear process. The nature of the wear pattern on the discs (with the most extensive wear taking place on surfaces normal to the direction of travel of the surface through the abrasive fluid) indicates that the effects of sliding, and thus particle-surface frictional effects, are also of lesser importance than particle impact events. For this reason it would seem that the erosive wear damage process of these insulator materials is likely to be largely mechanical, rather than electrical, in origin.

An approximate dependence of wear rate on $(\text{grain size})^{-1/2}$ is suggested (shown in Fig. 11), similar to that seen for fully dense hot-pressed and sintered 100% alumina materials.[22] However, treatment in accord with the supposition that wear proceeds by a 'stop–go' process, involving grain boundary microcracking and crack arrest at multiple grain boundary junctions and giving a wear rate proportional to $G/(G + G_0)$, also yields a straight line passing through the origin for $G_0 = 3$ μm (shown in Fig. 12). The wear rates for the zircon materials are similar to those for pure polycrystalline alumina of comparable grain size (Fig. 13), though the zircon wear is some 30% slower at each grain size. In view of the large glass content of the zircon materials this is surprising, but

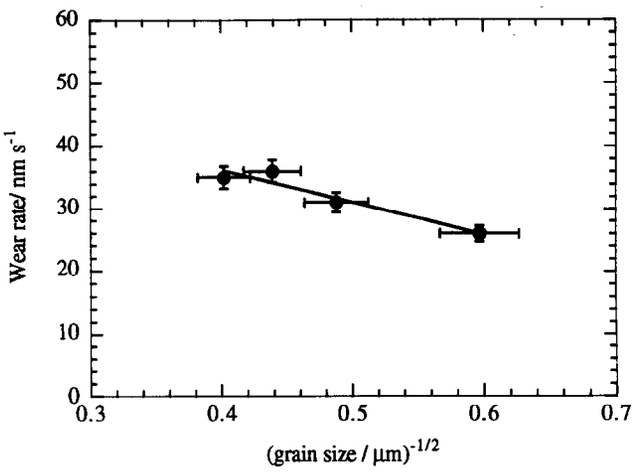

Fig. 11. Wear rate as a function of $(\text{grain size})^{-0.5}$.

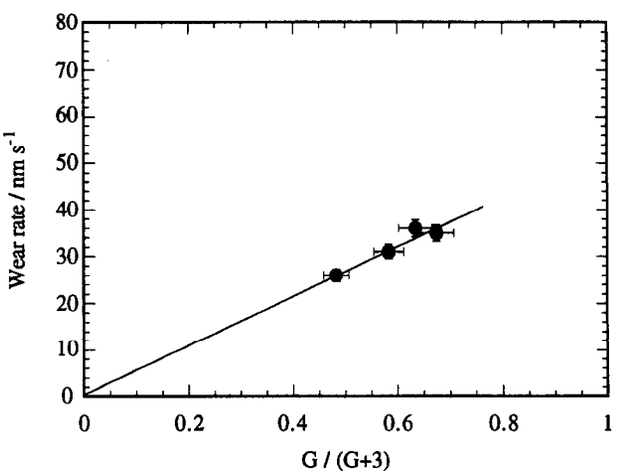

Fig. 12. Wear rate as a function of $G/(G+3)$.

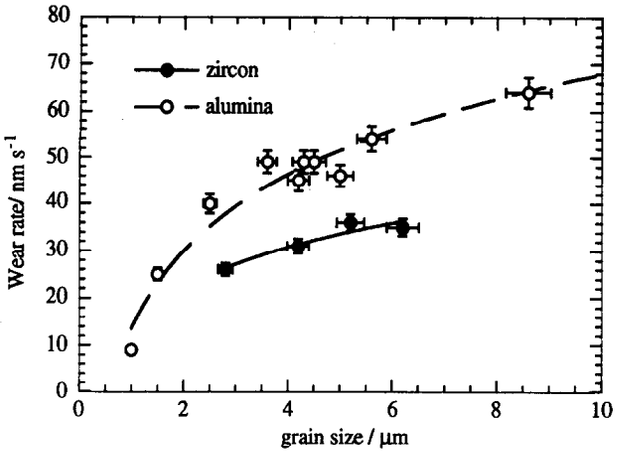

Fig. 13. Wear rate as a function of grain size for dense zircon and pure alumina materials.

preliminary wear rate data for sintered alumina materials containing 5 to 10% of a liquid-forming silicate system suggest that wear rate is insensitive to the intergranular glass content at this level.[28]

A second clear factor controlling wear rate is porosity: the relationship between pore fraction and wear rate shown by Fig. 7 for the three 6·2 μm zircon materials. Although there are only three points there is the suggestion that wear, by grain dislodgment, occurs preferentially at the edges of the pores. This is supported by Figs 8 to 10 which show the wear damage in Z4 material of 0·036 pore fraction.

On the basis of this study, it seems that fine-grained liquid phase sintered zircon materials will have low wet erosive wear rates, comparable with those of fine-grained sintered alumina materials, provided full density can be attained. Unlike the alumina materials, grain growth in zircon does not readily occur, which provides an added intrinsic advantage for this type of material. Densification is therefore predominantly the result of the combined processes of void filling by liquid, and particle rearrangement.

5 Conclusions

Two wear mechanisms appear to be responsible for the loss of material during the wet erosive wear of liquid phase densified zircon. One is probably a non-selective tribochemical dissolution of the zircon grains and intergranular glass phase in which the zircon grains are embedded. This process leads to a polishing action, and would not be expected to be related to the zircon grain size for material with a constant volume fraction of glass phase. Another, and probably dominant, factor with this group of zirconia materials is grain-size related, and seems likely to be a grain detachment process, occurring through localized microfracture and crack linking. The variations in wear rate seen within this set of materials are not explicable in terms of H or K_{1c}, because these are essentially constant. Porosity is an important additional factor and leads to considerable enhancement of wear rate. Exploration is being continued of the precise basis for, and form of, the quantitative relationship between the rate wear by grain detachment, and grain size, in materials of this type.

Acknowledgements

Gramcol Zircon Ltd, Stoke-on-Trent, UK, is thanked for the provision of zircon powders, and for assistance with particle milling and particle size analyses. Financial support from the Asturian Research Foundation to M. Miranda-Martinez is gratefully acknowledged. Dr. E. Gilbart provided invaluable technical assistance with powder hot-pressing.

References

1. Speer, J. A., Orthosilicates. Zircon, *Rev. Mineral.*, **5** (1980) 67–112.
2. Beretka, J., Bowman, R. G. & Brown, T., Studies on zircon pigments for ceramic glazes, *J. Aust. Ceram. Soc.*, **17** [2] (1981) 37–43.
3. Hathaway, A. J. C., Holmes, R. & Peters, R. Effective use of zircon opacifiers. *Ceram. Eng. Sci. Proc.*, **4**[11-12] (1983) 1036–46.
4. Adams, W. T., Zircon: from curiosity to commodity. *Am. Ceram. Soc. Bull.*, **68**[5] (1989) 1024–7.
5. Garnar, T. E., Zircon. *Am. Ceram. Soc. Bull.*, **69**[5] (1990) 888–90.
6. Ryshkewitch, E. & Richerson, D. W., *Oxide Ceramics: Physical Chemistry and Technology*. Academic Press Inc., Orlando, FL, 1985, 2nd Ed.
7. Butterman, W. C. & Foster, W. R., Zircon stability and the ZrO_2–SiO_2 phase diagram. *Am. Mineral.*, **52** (1967) 880–5.
8. Levin, E. M., Robbins, C. R. & McMurdie, H. F. (Eds), *Phase Diagrams for Ceramists*. American Ceramic Society Inc., Columbus, OH, 1964.
9. Curtis, C. E. & Sowman, H. G., Investigation of the thermal dissociation, reassociation, and synthesis of zircon. *J. Am. Ceram. Soc*, **36**[6] (1953) 190–9.
10. Boch, P., Kapelski, G. & Giry, J. P., Sintering properties of dissociated and reassociated zircon. *Proc. Br. Ceram. Soc.*, **38**, (1986) 149–60.
11. Anseau, M. R., Leblud, C. & Cambier, F., Reaction sintering of mixed zircon-based powders as a route for producing ceramics containing zirconia with enhanced mechanical properties. *J. Mater. Sci. Lett.*, **2**[7] (1983) 366–70.
12. Dörre, E. & Hübner, H., *Alumina — Processing Properties and Applications*. Springer Verlag, Berlin, 1984.
13. Evans, A. G. & Wilshire, T. R., Quasi static solid particle damage in brittle solids — I: Observations, analysis and implications. *Acta. Metall.*, **24** (1976) 939–56.
14. Fayeulle, S., Berroug, H., Hamzaoui, B. & Tréheux, D., Role of dielectric properties in the tribological behaviour of insulators. *Wear*, **162–164** (1993) 906–12.

15. Cho, S. J., Hockley, B. J., Lawn, B. R. & Bennison, J., Grain-size and *R*-curve effects in the abrasive wear of alumina. *J. Am. Ceram. Soc.*, **72**[7] (1989) 1249–52.
16. Rice, R. W. & Speronello, B. K., Effect of microstructure on rate of machining of ceramics. *J. Am. Ceram. Soc.*, **59**[7–8] (1976) 330–3.
17. Wiederhorn, S. M. & Hockey, B. J., Effect of material parameters on the erosion resistance of brittle materials. *J. Mater. Sci.*, **18** (1983) 766–89.
18. Wu, C. Cm., Rice, R. W., Johnson, D. & Platt, B. A., Grain size dependence of wear in ceramics. *Ceram. Eng. Sci. Proc.*, **6**[7–8] (1985) 995–1011.
19. Rice, R. W., Micromechanics of microstrutural aspects of ceramic wear. *Ceram. Eng. Sci. Proc.*, **6**[7–8] (1985) 940–58.
20. Marshall, D. B., Lawn, B. R. & Cook, R. F., Microstructural effects on grinding of alumina and glass ceramics. *J. Am. Ceram. Soc.*, **70**[6] (1987) C-139–40.
21. Gee, M. G. & Almond, E. A., The effects of surface finish on the sliding wear of alumina. *J. Mater. Sci.*, **25**(1A) (1990) 296–310.
22. Cho, S. J., Moon, H., Hockley, B. J. & Hsu, S. M., Wear transformation phenomenon in alumina during sliding. In *C-MRS Int. Symp. Meeting 1990*, ed. B. Wu., North-Holland, Amsterdam, 1991, vol. 5, pp. 387–9.
23. Miranda-Martinez, M., Davidge, R. W. & Riley, F. L., Grain size effects on the wet erosive wear of high purity polycrystalline alumina. *Wear*, **172** (1994) 41–8.
24. Davidge, R. W. & Riley, F. L., Grain size dependence of the wear of alumina. *Wear*, **186–187** (1995) 45–9.
25. Mendelson, M. I., Average grain size in polycrystalline ceramics. *J. Am. Ceram. Soc.*, **52**[8] (1969) 332–46.
26. Anstis, G. R., Chantikul, P., Lawn, B. R. & Marshall, D. B., A critical evaluation of indentation techniques for measuring fracture toughness: I. Direct crack measurements. *J. Am. Ceram. Soc.*, **64** (1981) 533–6.
27. Miranda-Martinez, M. & Riley, F. L., Wet abrasive wear of technical ceramics. *Br. Ceram. Trans. J.*, **90** (1991) 118–21.
28 Miranda-Martinez, M., Davidge, R. W. & Riley, F. L., The reduction of erosive wear rates of advanced technical ceramic materials. In *2nd International Conference Proceedings, Ceramics in Energy Applications*. The Institute of Energy, London, 1994, pp. 239–52.